Superconductive Tunneljunctions for X-ray Spectroscopy

P.A.J. de Korte[1], M.L. van den Berg[1], M.P. Bruijn[1], M. Frericks[1],
J.B. le Grand[1], J.G. Gijsbertsen[2], E.P. Houwman[2], and J. Flokstra[2]

[1] Laboratory for Space Research, Sorbonnelaan 2, 3584 CA Utrecht, the Netherlands
[2] University of Twente, Faculty of Applied Physics, Low Temperature Group, P.O. Box 217, 7500 AE Enschede, the Netherlands

ABSTRACT

Superconductive tunneljunctions are under development as detectors for X-ray astronomy in the 0.5-10 keV energy range, because of their potentially high energy resolution ($\delta E < 10$ eV) in combination with high detection efficiency.

Especially absorber-junction combinations offer the prospect of high energy resolution detectors with a high detection efficiency and a reasonable (~ 1 cm^2) size. The proximity effect between the Nb absorber and the Al trapping layer plays a dominant role. A study of the proximity effect in Nb/Al/Al_2O_3/Al/Nb junctions with different Al-layer, the trapping layer, thicknesses is presented.

1. INTRODUCTION

The pioneering efforts of the groups at the Paul Scherrer Institut[1,2] and the Technische Universität München[3] and their promising results, about 50 eV energy resolution at 5.9 keV, ignited the interest for research on superconducting tunneljunctions at various institutes.

Notwithstanding this broad effort the results on energy resolution have sofar not been improved.

The work in our group is directed to the development of detectors for X-ray spectroscopy of astronomical X-ray objects. To make these detectors attractive we require them to combine:
- high detection efficiency in the energy range $0.5 - 10$ keV
- good, about 10 eV, energy resolution
- some imaging, either by intrinsic imaging or by an array of individual detectors.

The need for reasonable efficiency requires a detector thickness of $20 - 30\,\mu$m Nb or an equivalent thickness of another superconductor. This requirement combined with the others excludes the use of simple junctions. Superconductive absorbers, read out by one or more superconductive junctions, possible by the use of quasiparticle trapping[4], are the most likely route to a successful detector.

The work in this paper is directed to the study of this quasiparticle trapping mechanism in junctions of Nb/Al/Al_2O_3/Al/Nb and is a precursor to the use of large absorbers, read out by small junctions.

2. THEORY

a. General

The response of superconductive junctions to X-ray photons is due to the creation of excess quasiparticles, which subsequently tunnel to the other film. The ultimate achievable energy resolution is given by the statistical variation on the number of created quasiparticles and is given by:

$$\delta E(\mathrm{FWHM}) = 2.355\,(F\epsilon E_x)^{\frac{1}{2}} \qquad (1)$$

 0-8194-0916-2/92/$4.00

with F the Fano factor, ϵ the mean energy required for the creation of a quasiparticle and E_x the energy of the X-ray photon. Calculations[5] performed for Nb yield $F = 0.22$ and $\epsilon = 1.75\ \Delta$, with Δ the bandgap energy for Nb.

Several papers have appeared on the initial loss of quasiparticles from the system due to localized heating by the absorption of the X-ray photon.[6,7,8] Calculations performed for Sn[8] indicate that this might account for a loss of about 50% of the quasiparticles in case of absorption of 5.9 keV X-rays. For Nb quantitative calculations do not exist, but qualitative arguments[7] indicate that the situation might be better than for Sn.

Other loss processes occur after the quasiparticle phonon system has relaxed to the bandgap, namely loss of quasiparticles and phonons from the system.

In figure 1 the various processes in this system are indicated. The loss processes and their impact on the signal level as well as on the energy resolution will be part of the discussions in the following paragraphs.

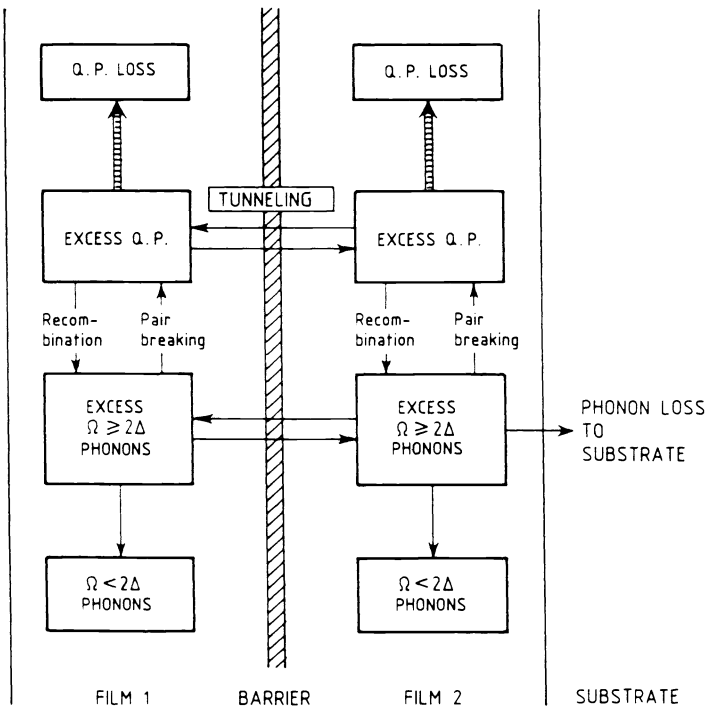

Fig. 1. Schematic of the quasiparticle phonon system stimulated by an X-ray photon creating excess quasiparticles and phonons. The situation is shown for a tunneljunction with two superconducting films on top of a substrate.

In this chapter some of the time constants governing the various processes are reviewed, since current literature is inconsistent. A crucial parameter is the time constant for tunneling, generally called the tunnel time τ_T. In line with the paper by Ginsberg[9] it follows that for a junction with two normal conducting films:

$$I = U/R_N \tag{2}$$

in which U equals the biasvoltage and R_N the normal resistance. For the current I also should hold:

$$I = qN\frac{1}{\tau_T} \tag{3}$$

in which N the number of charge carriers which can tunnel, q the electron charge and $\frac{1}{\tau_T}$ the tunneling probability. At $T \simeq 0$ the charge carriers N, which can tunnel, are

$$N = 2N_0VqU \tag{4}$$

with N_0 the density of states per spin direction per eV at the Fermi level and V the volume of the layer for which the tunnel time is calculated. So for a junction with normal conductive films the tunnel time equals

$$\tau_T^N = 2q^2N_0R_NV \tag{5}$$

In case tunneling between superconductors is considered this formula is changed for two reasons:

- Quasiparticles are split into electron-like ($k > k_F$) and hole-like ($k < k_F$) branches. Only the energy level of one of the branches corresponds to that with states at the other side of the barrier, thereby enhancing the tunnel time by a factor 2. This is illustrated in figure 2, which represents a superconductive junction in semiconductor representation.
- The density of states in a superconductor is strongly enhanced near the bandgap. This results in a correction factor to the tunnel time τ_T, which becomes smaller than one for relatively low bias voltages. This correction factor is independent of temperature as long as $kT \ll qU$.

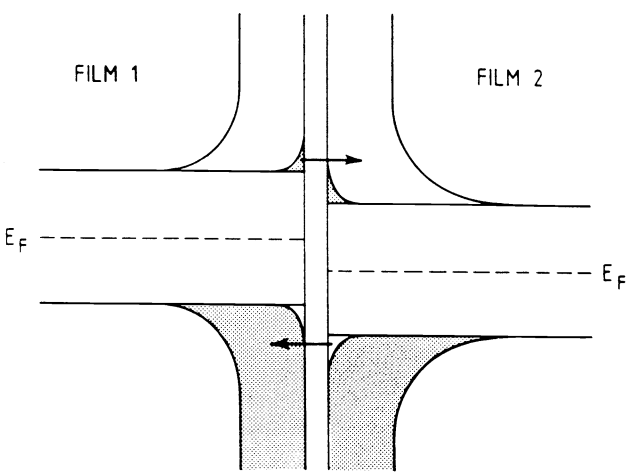

Fig. 2. The semi-conductor representation of a subgap biased junction with two superconductive films. This figure illustrates that the tunnel change for quasiparticles is reduced by a factor 2.

So the tunnel time for a superconductive junction with films of equal bandgap becomes:

$$\tau_T = 4q^2N_0VR_N\frac{[(\Delta + qU)^2 - \Delta^2]^{\frac{1}{2}}}{\Delta + qU} \tag{6}$$

Verification of this formula is possible by making use of the expressions for the thermal quasiparticle density[10]

$$n_{th} = 2N_0(2\pi\Delta kT)^{\frac{1}{2}}e^{-\Delta/kT} \tag{7}$$

and that for the thermal subgap current[11]

$$I_{th} = \frac{1}{qR_N}\frac{\Delta + qU}{[(\Delta + qU)^2 - \Delta^2]^{\frac{1}{2}}}(2\pi\Delta kT)^{\frac{1}{2}}e^{-\Delta/kT} \tag{8}$$

Since half of the thermal current comes from the film with volume V for which the tunnel time τ_T is calculated, the following relation holds:

$$qn_{th}V\frac{1}{\tau_T} = \frac{1}{2}I_{th} \tag{9}$$

Combining equations (7), (8) and (9) results again in expression (6) for τ_T.

The other, inconsistently treated, parameter is the temperature independent recombination rate R, defined as the average rate at which any single quasiparticle reacts with any other quasiparticle in an ensemble with a density equal to one. So the total rate at which recombination occurs equals:

$$\frac{1}{2}N(N-1)\frac{R}{V} \tag{10}$$

since $\frac{1}{2}N(N-1)$ is the number of ways we can make pairs out of N quasiparticles. The rate at which quasiparticles are converted into 2Δ phonons by recombination is[12]

$$-\frac{\partial N}{\partial t}\Big/_R \equiv \frac{N}{\tau_R} = N(N-1)\frac{R}{V} \tag{11}$$

since two QP's are destroyed by each recombination. In case of large N:

$$\tau_R = \frac{1}{nR} \tag{12}$$

with $n = \frac{N}{V}$. If one implements the thermal quasiparticle density (7) and the equation for τ_R from Kaplan[13] into equation (12) one obtains

$$R = \left(\frac{2\Delta}{kT_c}\right)^3\frac{1}{4N_0\Delta\tau_0} \tag{13}$$

When this is applied to recombination of excess quasiparticles N_{exc} one finds:

$$-\frac{\partial N_{exc}}{\partial t}\Big/_R = [2N_{exc}N_{th} + N_{exc}^2]\frac{R}{V} \tag{14}$$

of which the first term represents recombination of excess QP's with thermal QP's and the second self recombination. So for small numbers ($N_{exc} < N_{th}$) of excess QP's the time constant for the relaxation of excess QP's by recombination is twice as short as the recombination time τ_r calculated by Kaplan[13].

b. Proximity effect and quasiparticle trapping

The response of Nb-junctions with "thick" Al-layers adjacent to the barrier is dominated by QP trapping in the reduced bandgap region. The use of QP trapping for collection and faster tunneling of QP was first proposed by Booth et al.[4] The process is illustrated in figure 3. Excess QP created by X-ray stimulation scatter towards lower energies in the low bandgap region and get confined. This confinement in a small volume near the tunnel barrier reduces the tunnel time. The flow of QP and phonons in a junction with a low bandgap trapping layer is illustrated in figure 4, which forms the outline of a simple model used to interpret the data presented in this paper.

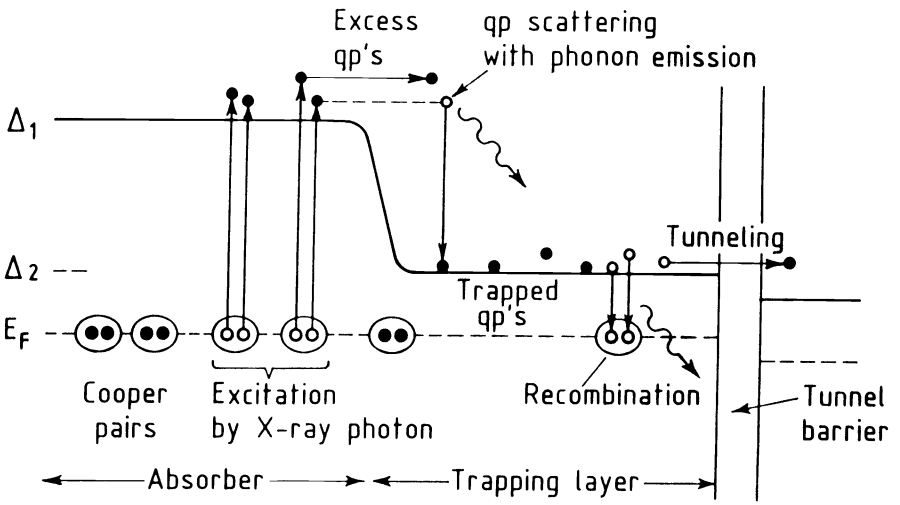

Fig. 3. Schematic of the trapping process[4] into a lower bandgap region caused by down scattering of the quasiparticle energy.

Since the counter electrode is covered by 20 nm of Al any excess QP's in this layer get instantaneously trapped in a region separate from the tunnel barrier. For the present model it implies that only signals are expected from X-ray absorption in the bottom layer and that backtunneling of excess QP's or phonons from the counter electrode can be neglected. This will be justified in a quantitative way later in the paper.

The bottom electrode in this model is split into two compartments, i.e.:

- One parallel and adjacent to the barrier with a reduced bandgap $\Delta_{\min}$
- One between the former compartment and the substrate with a bandgap equal to the one for bulk Nb, i.e. Δ_B.

In both compartments we assume a QP-phonon system governed by recombination and pair breaking as described by the Rothwarf-Taylor equations. In the transport between the two compartments the phonon transport is neglected, since it contains only a small fraction of the energy transport between both compartments. The loss of phonons from the system is described by the phonon trapping factor according to Kaplan[14]. For the low bandgap compartment the transmissivity for phonons at either side has been taken equal to one. For the bulk bandgap compartment the transmissivity equals 0.34 at the Nb/SiO_2 interface and 1.0 between both compartments. Loss of phonons by decay has been neglected.

Loss of QP's from the system is considered only for the bulk bandgap compartment. This time constant is actually the only free parameter of the model, since all other parameters can be derived from actual measurements and models.

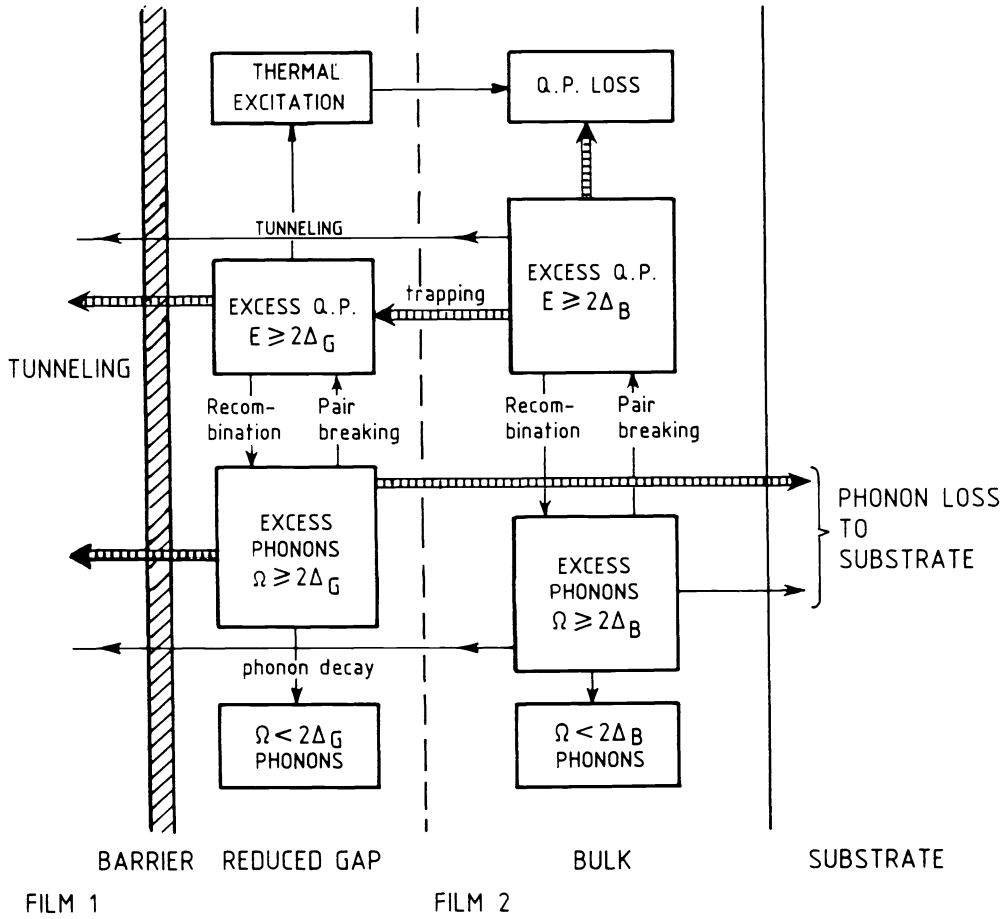

Fig. 4. Schematic of the quasiparticle phonon system stimulated into non-equilibrium by an X-ray photon. The situation is shown for a tunneljunction with a trapping layer in the bottom electrode.

QP's can however also get lost from the low bandgap region, since the thermal energy kT of the QP's is not too different from the depth, $\Delta_B - \Delta_{min}$, of the trapping compartment. So part of the QP's in the trapping layer are not confined and can get lost through the QP loss mechanism in the bulk bandgap compartment. This effect has been included in the model.

The key parameter in this model is the trapping time into the low bandgap compartment. This time constant for scattering towards a lower bandgap region is given by Kaplan[13]. For small energy differences δE, compared to the bandgap energy, and for a BCS density of state distribution the following approximation holds:

$$\tau_S \simeq (\delta E)^{-3.5} \tag{15}$$

For an exact solution the density of states as function of energy and position perpendicular to the barrier, in the reduced bandgap region, is required. This information combined with Kaplan's[13] general equation on QP scattering results in the trapping time.

This calculation has recently be performed by Golubov and Houwman[15] based on the earlier work by Golubov[16,17] on the proximity effect. Golubov characterizes this effect by two proximity parameters γ_m and γ_B. The behaviour of the order parameter near the S'S interface, defined by γ_m and γ_B, is shown in

figure 5. In our case S′ is the Al-layer and S the Nb layer. The parameters $\xi_{S'}$ and ξ_S are the coherence length in superconductors S′ and S. By solving the Usadel equations in the S′ and S region for $d_{s\prime} < \xi_{s\prime}$ and $d_s > \xi_s$ the required superconducting properties can be determined.

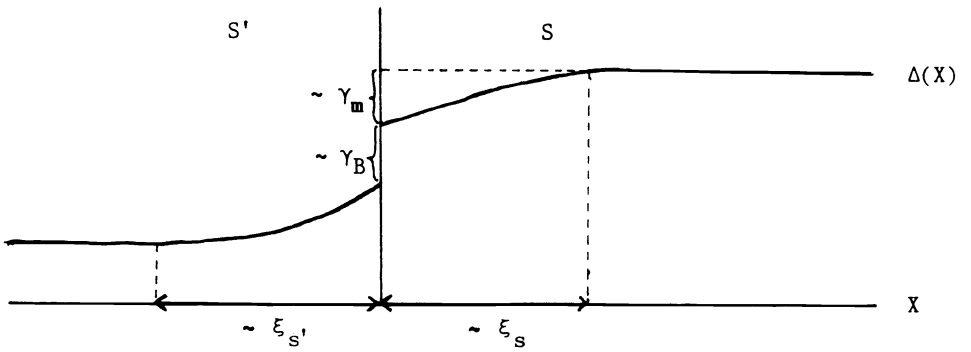

Fig. 5. Behaviour of the order parameter $\Delta(x)$ at an interface between two superconductors S and S′. The behaviour is characterized by the two proximity parameters γ_m and γ_B.

For Nb/Al junctions in which the Nb and Al-layer are sputtered in one run, study of the I-V characteristics for junctions with different layer thicknesses of Al have shown that $\gamma_B \simeq 0$, so that only γ_m describes the proximity effect in this case.

3. EXPERIMENTAL DATA

In order to investigate the influence of QP trapping on the performance of junctions as X-ray detectors a series of $Nb/Al/Al_2O_3/Al/Nb$ junctions have been produced with different Al-layer thicknesses in the bottom electrode. So far only 50 μm size junctions have been measured. The geometry of the devices is shown in figure 6.

The size of the electrodes equals $70 \times 70 \times 0.3$ μm^3 and $60 \times 60 \times 0.165$ μm^3 for the bottom and counter electrode, respectively. Both electrodes have a long connecting lead of 5 μm width. The counter electrode has been covered with 20 nm Al.

The Al-layers at the barrier range from 5 to 25 nm for the bottom electrode and equals 3 nm for the counterelectrode. The most useful data are given in the following table.

Table 1 Junction characteristics

Wafer	Rn (Ω)	Al-thickness (nm)	V_G (4 K) (mV)	Δ_{min} (1.5 K) (mV)
PROX 4	0.44	5	2.73	1.37
PROX 3	0.57	10	2.58	1.21
HG@7.2	0.16	15	2.54	1.17
PROX 2	0.58	20	2.40	1.02
PROX 1	0.48	25	2.30	0.93

The bandgap value of the counter electrode Δ_{max} (1.5 K) equals about 1.4 meV. Since both layers have been sputtered at ambient temperature they have a typical resistance ratio $RRR \simeq 5$.

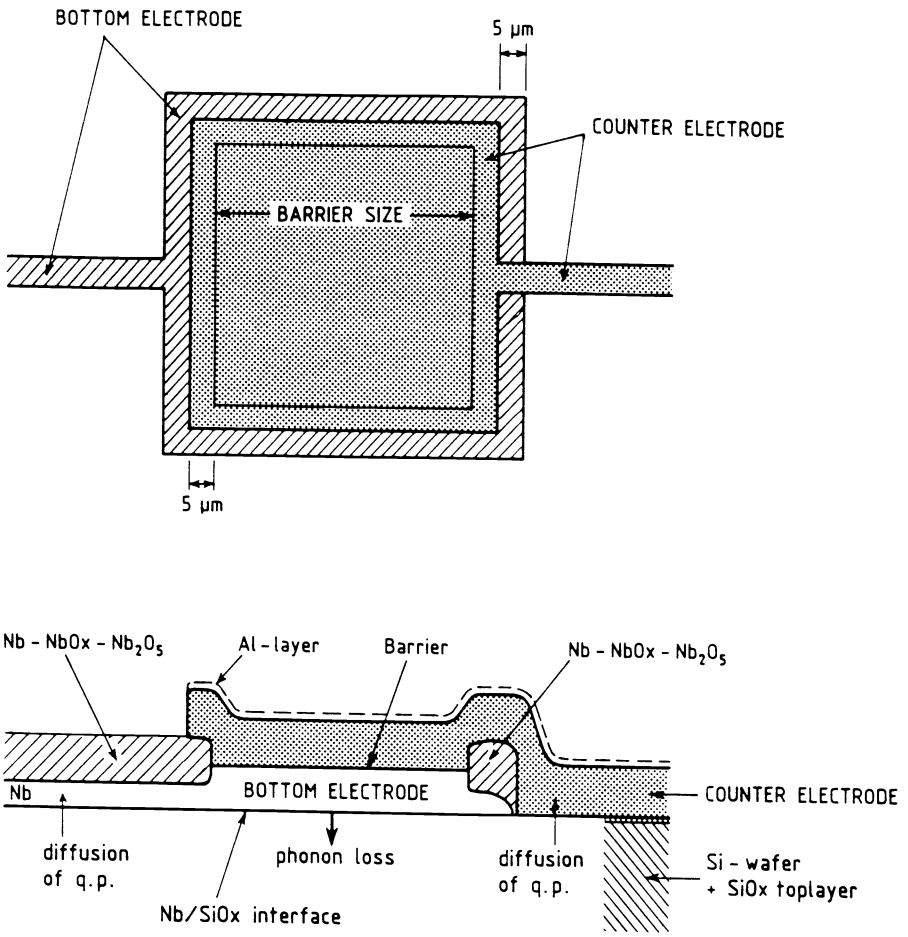

Fig. 6. Geometry of the $Nb/Al/Al_2O_3/Al/Nb$ junctions.

So far only X-ray measurements have been performed on 50 μm junctions of the first three wafers in the table. These measurements are performed by stimulation with 5.9 keV X-rays from an ^{55}Fe radioactive source. The junctions are biased at about 0.2-0.4 mV by a current source with voltage stabilization. The X-ray induced excess current in the junction is amplified by a cold charge sensitive preamplifier with a feedback capacitance of 1 pF and a bandwidth limited rise time of approximately 350 nsec.

In figure 7 four pulse height spectra are shown, two for the PROX 3 wafer, 10 nm Al, and two for the HG@7.2 wafer, 15 nm Al. The two spectra for both wafers have been taken at different temperatures. The axes for the pulse height are in volts. For both cases one volt corresponds to approximately 90.000 electrons of tunneled charge. The measured pulse shapes for all runs are consistent with a signal decay time shorter than about 350 nsec.

Characteristics of the data in figure 7 and the other available data are given in Table 2.

The peak positions in the above table are normalized to an expected number of excess QP equal to $2.4\,10^6$ for an X-ray of 5.9 keV. The peak position represents the highest pulse height feature in the spectrum. Other information, which can be extracted from the data is the countrate, i.e. $\simeq$ 190 counts/sec for HG@7.2 and $\simeq$ 65 counts/sec for PROX 3.

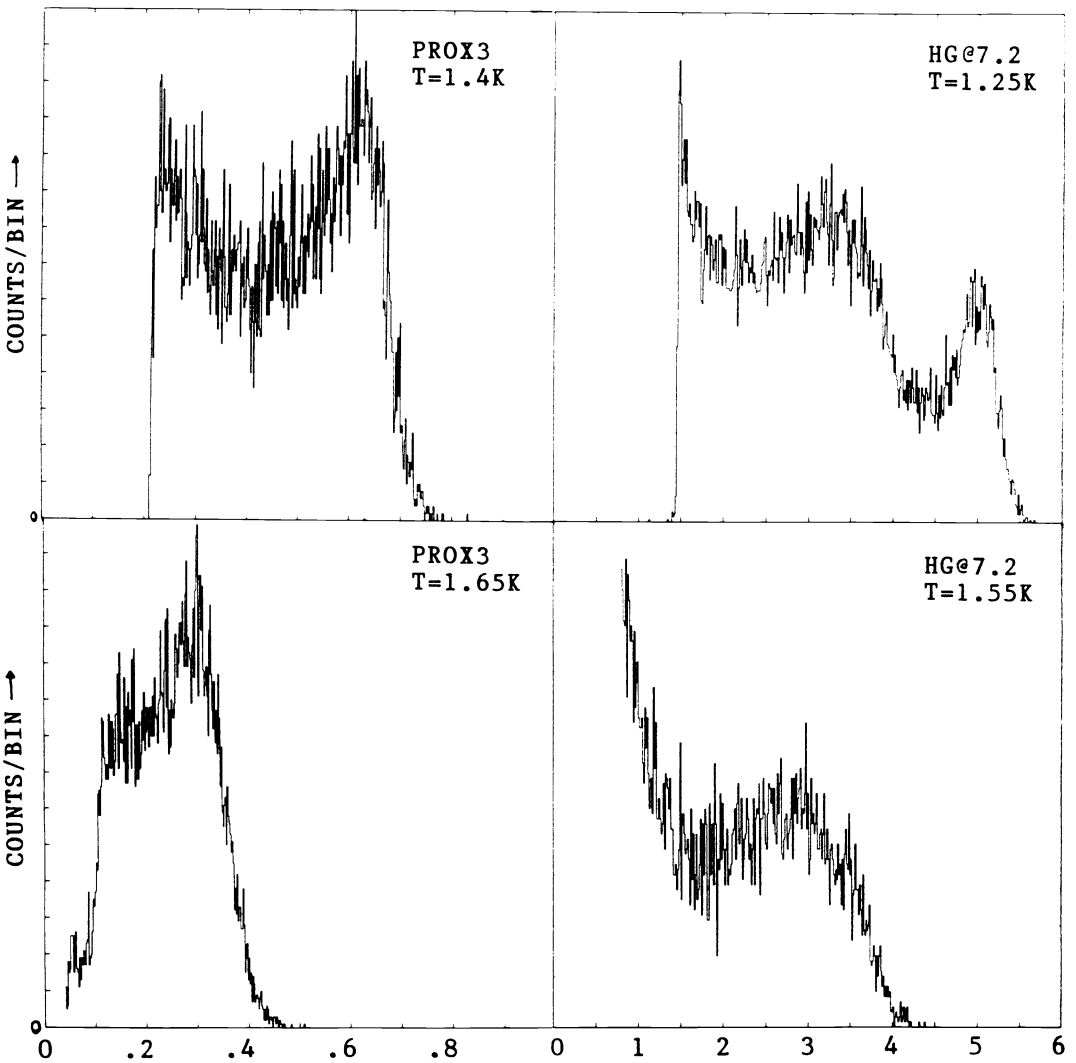

Fig. 7. Measured pulse height distributions for the PROX 3 and HG@7.2 wafer. For each device the spectra are given at two temperatures. The pulse height is given in volts. In both cases 1 V corresponds to a tunneled charge of about 90.000 electrons.

Table 2 Spectral information

PROX 4		HG@7.2		PROX 3	
(K)	PEAK (%)	T(K)	PEAK (%)	T(K)	PEAK (%)
1.5	2.6	1.25	20	1.40	2.3
		1.40	15	1.43	2.5
		1.55	11	1.55	1.7
		1.64	8	1.65	1.1
		1.75	7	1.75	0.6
		1.88	6		

4. DISCUSSION AND INTERPRETATION

The data interpretation along the model explained in the theory section requires the determination of its time constants. Based on the information in table 1 and the work of Golubov and Houwman[15] the trapping times for the various wafers can be determined. Also given are the relevant tunnel times for the bottom layer as well as for the trap. Based on the work of Golubov the width of the trapping layer is estimated as the thickness of the Al-layer plus $1.5\xi_S$, which in case of Nb equals 60 nm. The most relevant parameters are given in table 3.

Table 3 Junction parameters

Wafer	γ_m	τ_{trap} (nsec)	τ_T^{Nb} (μsec)	τ_T^{Tr} (μsec)	$\delta\Delta$ (meV)
PROX 4	0.2	770	5	1.1	0.08
PROX 3	0.4	100	6.5	1.5	0.24
HG@7.2	0.6	36	1.8	0.5	0.28
PROX 2	0.8	20			

$\delta\Delta$ in the above table is the energy gap difference between the two compartments in the bottom electrode and is required to calculate the fraction of QP in the trapping layer, which is not confined due to thermal excitation. This fraction is calculated by folding the Fermi-Dirac distribution with a constant density of states, a crude approximation to density of state calculations at the S'S interface by Golubov.

From the data in this table it is derived that:

1. The trapping time in the Al-layer of the counter electrode equals 11 nsec. This is a value deduced from PROX 2 data and corrected for the thickness ratio of bottom and counter electrode.
   The maximum event fraction which can therefore be expected from the counter electrode equals 0.3% for PROX 3 and 1% for HG@7.2. So the conclusion that the counterelectrode is effectively a sink to excess QP's and phonons is justified.
2. Trapping plays only a very limited role for PROX 4, since the trapping time is long and $\delta\Delta = 0.08$ meV is smaller than kT, so that a large fraction of the particles in the trap are not really confined.

On the basis of the values in table 3 we have made a coarse fit to the peak values given in table 2. The result is shown in figure 8 for the PROX 3 and HG@7.2 data. The τ_{loss} time constant is adjusted to fit the lowest temperature datapoint on each data set. The τ_{loss} values are 25 and 30 nsec for the PROX 3 and HG@7.2 data, respectively. The signal decay times calculated in this model are consistent with a measured decay time shorter than 350 nsec.

From the fits it is apparent that the loss time in the high bandgap region of the bottom electrode is extremely short. If one performs the same analysis on the PROX 4 datapoint a loss time of 80 nsec is calculated. This discrepancy is not explained.

Given these short loss times the energy resolution of the junctions is strongly influenced by local variations in the τ_{loss} time and edge effects. The QP cloud diameter 30 nsec after creation equals about 25 μm. The strong influence of edge effects is apparent from the measured countrates, i.e. 190 and 65 counts/sec for HG@7.2 and PROX 3, respectively. The expected countrates for the $70 \times 70 \times 0.3$ μm^3 bottom electrodes are 530 and 170 counts/sec, respectively. So the measured events originate from a central area of about 40 μm square.

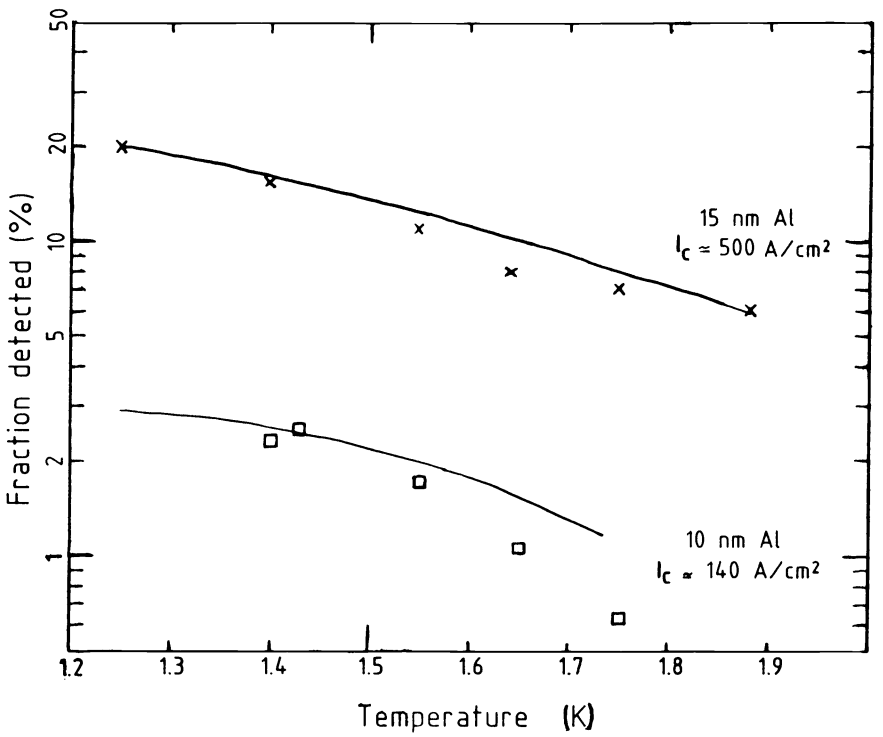

Fig. 8. Peak positions of the pulse height distributions as measured for the PROX 3 and HG@7.2 wafer for various temperatures. Also is drawn a model fit to the data.

No additional QP loss time had to be incorporated in the QP trap near the barrier. Given the fraction of non-confined QP in the trap, due to thermal excitation, a lower limit can be set on any QP loss in the trap itself, i.e. about 400 nsec. A confirmation of this conclusion can be obtained by measuring pulse shapes with a faster amplifier.

So on the basis of the above discussion on the QP loss times it is concluded that the QP loss does not originate in the bulk but originates predominantly from trapping at the Nb-SiO_2 interface and at the edges made by anodization. This is not inconsistent with the severe bandgap reduction in Nb due to surface oxidation.[18] This trapping mechanism has been shown to be very efficient for relatively small bandgap reductions.

5. CONCLUSIONS

The results obtained on Nb junctions with Al-layers of various thicknesses indicate that:

- quasiparticle trapping is quite an efficient process in Nb junctions with Al-layers of 10 nm and thicker.
- the proximity model by Golubov and Houwman[15] can explain the present data quite well.
- Nb junctions suffer from the bandgap reduction at oxidized and anodized surfaces. Without any special attention extremely fast loss processes, about 30 nsec, are present.

6. ACKNOWLEDGEMENTS

The authors are grateful to A.A. Golubov for the discussions on the proximity effect and quasiparticle trapping. These investigations form also part of the program of the Foundation for Fundamental Research on Matter (FOM) and have been supported by the Netherlands Technology Foundation (STW).

7. REFERENCES

1. D. Twerenbold and A. Zehnder, "Superconducting Sn/Sn-oxide/Sn tunneling junctions as high-resolution X-ray detectors", J. Appl. Phys. **61**, pp. 1-7, Jan. 1987.

2. A. Zehnder, "Cryogenic Detectors", Festi-Val Festschrift for V. Telegdi, K. Winter, ed. Elsevier Science Publ. BV, 1988.

3. H. Kraus, F. von Feilitzsch, J. Jochum, R.L. Mössbauer, Th. Peterreins and F. Pröbst, "Quasiparticle trapping in a superconductive detector system exhibiting high energy and position resolution", Phys. Lett. B. **231**, pp. 195-202, Nov. 1989.

4. N.E. Booth, "Quasiparticle trapping and the quasiparticle multiplier", Appl. Phys. Lett. **50**, pp. 293-295, Febr. 1987.

5. N. Rando, A. Peacock, A. van Dordrecht, R. Engelhardt, C. Foden, B.G. Taylor, P. Garé, J. Lumley, and C. Pereira, "The properties of Niobium superconducting tunneling junctions as X-ray detectors", Nucl. Instr. & Meth. A. **313**, pp. 173-195, 1992.

6. D. Van Vechten and K.S. Wood, "The probability of quasiparticle self-trapping due to the localized energy deposition in non-equilibrium tunneljunction detectors", Phys. Rev. B **43**, p. 12852, 1991.

7. N.E. Booth, R.J. Gaitskell, D.J. Goldie, C. Patel and G.L. Salmon, "Single crystal superconductors as X-ray detectors", Proc. of the workshop: X-ray detection by superconducting tunneljunctions, Napels, 12-14 Dec. 1990, Eds. A. Barone, R. Cristiano & S. Pagano, World Scientific, 1991.

8. W. Rothmund, "Quasiparticle and phonon relaxation after energy deposition in superconductors", Proc. of the workshop: X-ray detection by superconducting tunneljunctions, Napels, 12-14 Dec. 1990, Eds. A. Barone, R. Cristiano & S. Pagano, World Scientific, 1991.

9. D.M. Ginsberg, "Upper limit for quasiparticle recombination time in a superconductor", Phys. Rev. Lett. **8**, pp. 204-207, March 1962.

10. P.W. Epperlein, K. Lassmann, and W. Eisenmenger, "Quasiparticle recombination time in superconducting Tin and normal electronic density of states at the Fermi surface from tunneljunctions experiments", Z. Physik B. **31**, pp. 377-384, 1978.

11. W. Eisenmenger, "Superconducting tunneljunctions as phonon generators and detectors", Physical Acoustics, **XII**, Eds. W.P. Mason and R.N. Thurston, Academic Press, 1976.

12. K.E. Gray, "Steady state measurements of the quasiparticle lifetime in superconducting aluminium", J. Phys. F.: Metal Phys. **1**, pp. 290-308, 1971.

13. S.B. Kaplan, C.C. Chi, D.N. Langenberg, J.J. Chang, S. Jafarey, and D.J. Scalapino, "Quasiparticle and phonon lifetimes in superconductors", Phys. Rev. B. **14**, pp. 4854-4873, 1976.

14. S.B. Kaplan, "Acoustic matching of superconducting films to substrates", J. Low Temp. Phys. **37**, pp. 343-365, 1979.

15. A.A. Golubov and E.P. Houwman, "Quasiparticle relaxation rates in a spatially inhomogeneous superconductor", to be submitted to Physica A.

16. A.A. Golubov and M.Yu. Kupriyanov, "Theoretical investigation of Josephson tunneljunctions with spatially inhomogeneous superconducting electrodes", J. Low Temp. Phys. **70**, pp. 83-130, 1988.

17. A.A. Golubov and M.Yu. Kupriyanov, "Josephson effect in SNINS and SNIS tunnel structures with finite transparency of the SN boundaries", Sov. Phys. JETP **69**, pp. 805-812, 1989.

18. J. Halbritter, "On the oxidation and on the superconductivity of Niobium", Appl. Phys. A **43**, pp. 1-28, 1987.